miR-206 regulates alveolar type II epithelial cell Cx43 expression in sepsis-induced acute lung injury

JIAWEI ZHOU[1], YUMEI FU[1], KAI LIU[1], LINYI HOU[2] and WENKAI ZHANG[2]

[1]Department of Thoracic Surgery, Shanxi Medical University; [2]Department of Intensive Care Unit, Second Hospital of Shanxi Medical University, Taiyuan, Shanxi 030001, P.R. China

Received July 30, 2018; Accepted March 29, 2019

DOI: 10.3892/etm.2019.7551

Abstract. The present study investigated the relationship between connexin 43 (Cx43) expression in alveolar type II epithelial cells (ATII) and alveolar air-blood barrier permeability, and the effect of microRNA-206 (miR-206) on the expression of Cx43 in sepsis-induced acute lung injury. For the *in vivo* study, rats were divided into the sham, caecum ligation and perforation (CLP), CLP+Cx43 inhibitors (Cx43-In) and CLP+miR-206 analogs (miR-206-Mi) groups. CLP method was used to prepare an acute lung injury model of sepsis. Following successful modeling, lung tissue was collected for hematoxylin and eosin (HE) staining, and the wet to dry weight ratio (W/D) and protein content in bronchoalveolar lavage fluid (BALF) were detected. Cx43 expression in lung tissue was determined by immunohistochemistry and western blot analysis. Additionally, miR-206 and Cx43 expression levels in lung tissue were detected by reverse transcription-quantitative polymerase chain reaction. Rat ATII cells were cultured in Transwells plates to form monolayers, then treated with Cx43 mRNA inhibitors or miR-206 analogs. The cell monolayers were then stimulated with lipopolysaccharide and their permeability was evaluated by detecting fluorescein-labeled dextran at the lower chamber of the Transwells. The dual luciferase reporter gene assay was used to investigate whether miR-206 targeted the 3' untranslated region of Cx43 mRNA to regulate Cx43 expression, thereby regulating the permeability of the alveolar air-blood barrier. Results demonstrated that the CLP method induced damage to the alveolar structure, thickened the alveolar wall, caused hyperemia and hemorrhage in the pulmonary interstitium and caused infiltration of inflammatory cells. Edema in the pulmonary interstitium and alveolar space, exudation of neutrophilic granulocyte and pink edema fluid in alveolar cavities were also observed. W/D ratio, the BALF protein content, and expression of Cx43mRNA and Cx43 were increased significantly, whilst miR-206 expression decreased compared with the control group. The lung tissue inflammatory response was attenuated, and the W/D ratio and BALF protein content decreased in the Cx43-In and miR-206-Mi groups compared with the CLP group. Moreover, Cx43 mRNA and protein expression were decreased significantly in the Cx43-In and miR-206-Mi groups. In addition, the dual luciferase reporter gene assay determined that the untranslated region of Cx43 mRNA had a complementary sequence to miR-206. Of note, Cx43 mRNA expression in the miR-206-Mi group was not significantly decreased *in vitro*. In conclusion, the increase in ATII cell Cx43 expression during sepsis-induced acute lung injury resulted in an increase in the permeability of the alveolar air-blood barrier. miR-206 targeted the Cx43 mRNA 3'untranslated region to downregulate Cx43 expression, which further improved the permeability of the alveolar air-blood barrier.

Correspondence to: Dr Wenkai Zhang, Department of Intensive Care Unit, Second Hospital of Shanxi Medical University, 382 Wuyi Road, Taiyuan, Shanxi 030001, P.R. China
E-mail: 13994206729@163.com

Key words: microRNA-206, connexin 43, alveolar type II epithelial cell, sepsis, acute lung injury

Introduction

Sepsis is a systemic inflammatory response syndrome caused by infection, involving the whole body, with the lungs being one of the first organs affected. Acute lung injury (ALI) caused by sepsis is a serious disease that can further develop into life-threating acute respiratory distress syndrome. Current treatment measures include protective mechanical ventilation, surfactant replacement therapy, glucocorticoids and nitric oxide inhalation; however, they do not significantly improve the prognosis of ALI, and the mortality rate is high at 30-40% (1).

Due to the air-blood membrane barrier function in normal lung tissue, the protein-rich liquid cannot leak freely into the alveolar space or pulmonary interstitium (2). In sepsis-induced ALI, the lung microvascular endothelial cells and alveolar epithelial cells are impaired. This increases the permeability of the alveolar air-blood barrier leading to edema of alveolar space and the pulmonary interstitium, pulmonary hemorrhage and the infiltration of a large number of neutrophils and alveolar macrophages, which exacerbates injury. The increased permeability of the alveolar air-blood barrier is a crucial component of ALI with the alveolar epithelial barrier function regarded as more important than the microvascular endothelial barrier. Gorin *et al* (3) determined that the barrier function of the alveolar epithelium was stronger than the vascular endothelium. Even under normal conditions, injury to the barrier function of

alveolar epithelium can lead to the occurrence of pulmonary edema. Matthay *et al* (4) demonstrated that the alveolar epithelial barrier function is the most crucial in the pathogenesis of ALI; the damage degree of alveolar epithelial barrier determined the condition of the ALI patients, and the recovery of epithelial barrier function determined the prognosis of patients.

A previous study demonstrated that the permeability of the alveolar membrane barrier largely depends on the intercellular connections in the paracellular pathway (5). Intercellular connections include three major junction complexes: adherence junction, tight junction and gap junction (GJ). A GJ is a special membrane channel structure that exists between two adjacent tissue cells and consists of two mirror-symmetric connexons (Cn). The lung tissue epithelial cells mainly express Cx43, Cx37, and Cx40, of which Cx43 is the major connexin in ATII cells (6). The GJ consisting of connexin Cx43 forms a gap junction channel (GJC) between cells. Substances with a size of ~1,000 Da, such as direct dispersion of hydrophilic ions, molecules, metabolites or signal transduction molecules, can pass through; thereby GJCs serve a gating role, and regulate the transport and distribution of ions, currents, and low molecular weight metabolites. This connection between ATII cells ensures the integrity of the alveolar air-blood barrier. When the expression of Cx43 is upregulated, the channel and communication function of GJs is greatly changed, so that the macromolecular substances that could not initially pass through can now smoothly cross into the alveolar cavity and pulmonary interstitium affecting the permeability of the alveolar air-blood barrier. A study reported that post-traumatic cerebral edema is associated with Cx43 expression and that blocking Cx43 reduces the number of gap junctions formed between astrocyte, which in turn reduces glutamate release and alleviates brain edema (7). Previous research on intercellular GPs have focused on the development and metastasis of tumors, cardiovascular diseases and organ development but the relationship between Cx43 protein and lung injury is less studied. Therefore, exploring the relationship between Cx43 and alveolar air-blood barrier permeability has important theoretical significance for the prevention and treatment of sepsis-induced ALI.

microRNA (miRNA) is a small non-coding gene expression regulator that mediates gene silencing following transcription. miRNA regulates mRNA expression via two regulatory mechanisms. One mechanism occurs when the miRNA is completely complementary to the target mRNA and protein expression is reduced via degradation of the target mRNA. The other mechanism involves non-complementary miRNA and target mRNA, where mRNA translation is inhibited, reducing the protein expression of the target protein but mRNA expression is not affected. miRNA-206 (miR-206) is a multifunctional miRNA, that is widely involved in various pathological and physiological processes in different tissues. For example, miR-206 was involved in the development of bronchoalveolar dysplasia by down-regulating fibronectin 1 in premature infants with the disease (8). It also downregulates brain-derived neurotrophic factor expression leading to neurological dysfunction of airway smooth muscle, which in turn causes lung inflammatory disease (9). Zhang *et al* (10) determined that miR-206 regulates vesicle-associated membrane protein expression by direct inhibition of the target gene and affects the secretion of surfactants by ATII cells. Therefore miR-206 is widely involved in the regulation of lung function.

It has been demonstrated that miR-206 inhibits breast cancer cell proliferation and metastasis by targeting the Cx43 gene 3'untranslated region (UTR) 478-484 and 1609-1615 sequences, blocking Cx43 expression (11). Anderson *et al* (12) identified that miR-206 was involved in skeletal muscle differentiation by downregulating Cx43 expression at the post-transcription level. Kin *et al* (13) demonstrated that miR-206 regulates Cx43 expression and participates in the induction of C2C12 myoblast differentiation. However, further investigation is required to determine whether the ATII cell barrier function is regulated by miR-206 via targeting the Cx43 gene in sepsis-induced ALI.

The present study utilized the miRNA target gene prediction software TargetScan (http://www.targetscan.org/) to identify that the 3'UTR of the Cx43 gene had complementary sequences to miR-206 at sites 466-473 and 1580-1587. Therefore, dual luciferase reporter gene assay was used to determine the effects of Cx43 on the regulation of the ATII barrier in sepsis-induced ALI *in vivo* and *in vitro*. It was hypothesized that miR-206 targeted Cx43 mRNA to regulate the permeability of the ATII barrier.

Materials and methods

Animals and cells. A total of 32 male C57BL/6 mice (4-6 weeks; 18-22 g weight) were provided by the Physical Laboratory Animal Center at the Shanxi Medical University [animal license: SCXK (jin) 2015-0001] and raised in a specific-pathogen-free animal laboratory. The mice were placed on clean bedding in a room with laminar airflow, the indoor temperature was controlled at 18-22˚C, the humidity was 50-60% and the mice were given access to food and water *ad libitum*. Rat ATII cells RLE-6TN were purchased from Shanghai Baili Biotechnology Co., Ltd., and 293T human embryonic kidney cells were purchased from the Type Culture Collection of the Chinese Academy of Sciences.

Reagents. Transwell plates were purchased from Corning, Inc. fluorescein-labeled dextran (FITC-dextran; cat. no. FD40S) and lipopolysaccharide (LPS) were purchased from Sigma-Aldrich (Merck KGaA). Fetal bovine serum (FBS) was purchased from Cellmax. Cx43 mRNA inhibitors, an siRNA, (antogamir; 5'-CUCUCGCUCUGAAUAUCAUTTAUGAUAUUCAGAGCGAGAGTT-3') and miR-206 mimics (agomir; 5'-UGGAAUGUAAGGAAGUGUGUGGACACACUUCCUUACAUUCCAUU-3') were purchased from Shanghai Gemma Pharmaceutical Technology Co. Ltd. Cx43 antibody was purchased from Proteintech, Inc. and GAPDH antibody was purchased from Bioworld Technology, Inc. Dulbecco's modified Eagle's medium (DMEM) containing sodium pyruvate, sheep anti-rabbit horseradish peroxidase-conjugated immunoglobulin G antibodies, bovine serum albumin (BSA), coomassie brilliant blue G-250 and bicinchoninic acid BCA protein quantitative kits were all purchased from Wuhan Boster Biological Technology, Ltd. TRIzol total RNA extraction kit, Fast Quant RT kit with gDNA and SuperReal fluorescence Quantitative Premix were purchased from Tiangen Biotech Co., Ltd. M5 Pre-stained Protein Ladder was purchased from PCM Biotechnology Co., Ltd. Histostain™-Plus kit (cat. no. SP-0022) was purchased

Figure 1. Sepsis-induced acute lung injury induced by caecum ligation and perforation method. Surgical preparation of mice was as follows: (A) Disinfection, (B) incision of abdomen midsection, (C) exposure of the caecum, (D) ligation in the proximal end, (E) perforation in the distal end and extrusion of intestinal contents and (F) return to the caecum and closure of the abdominal cavity.

from Beijing Boaosen Biotechnology Co., Ltd. All the primers were purchased from the Sangon Biotech Co., Ltd.

Mouse sepsis model. Mice were randomly divided into 4 groups: Sham, caecum ligation and perforation (CLP), CLP+Cx43 inhibitors (Cx43-In) and CLP+miR-206 mimics (miR-206-Mi) groups. A modified experimental paradigm of CLP was used to induce ALI based on methods described in a previous study (14). In brief, mice were anesthetized with intraperitoneal injection of 3.5% chloral hydrate (10 ml/kg). The caecum was exposed by midline incision then the proximal caecum was ligated with silk thread. The distal caecum was punctured with a 20 ml syringe needle, squeezing out any intestinal contents, then placed back into the abdominal cavity. The abdominal cavity was closed by suturing the wound (Fig. 1). In the sham group, the caecum was only turned by median incision, without ligation and perforation.

Animal treatments. Mice in the Cx43-In group were injected in the tail vein with 125 μl Cx43 antagomir (16.5 μg/μl) and the mice in the miR-206-Mi group were injected with 125 μl miR-206 agomir (16.5 μg/μl). The mice in the sham and CLP groups were injected with 125 μl normal saline. The sepsis model was established after 24 h of intervention.

Protein content in bronchoalveolar lavage fluid (BALF). Mice were sacrificed via cervical dislocation 6 h following modeling. The chest was immediately opened, the right main bronchus ligated and endotracheal intubation was performed with intravenous indwelling needle to tracheal bifurcation. Then sterile and cooled PBS (0.3 ml) was used to lavage the left lung, pumping 3 times, and then BALF was gently drawn. The process was repeated 3 times and the recycled liquid stored was in a centrifuge tube in ice water temporarily. The recovery rate was ~75%. The BALF was centrifuged at 25,000 x g for 10 min at 4˚C, then the supernatant was stored at -20˚C prior to protein content analysis using coomassie brilliant blue stain.

Hematoxylin and eosin staining. The middle lobe of the right lung was fixed in 4% paraformaldehyde at room temperature for 24 h, dehydrated with alcohol, embedded in paraffin, cut into 0.5-0.8 μm sections then dewaxed. The sections were stained with hematoxylin for 10 min at room temperature. Then they were placed in eosin for 5 min at room temperature. The sections were observed under a fluorescent microscope at magnifications of x100 and x400.

Wet to dry weight ratio (W/D). The lower lobe of the right lung tissue was blotted with filter paper to remove any surface moisture then weighed to get wet weight (W). Samples were dried at 50˚C in an oven for 48 h to a constant weight, and then weighed to get the dry weight (D) The W/D was then calculated.

Reverse transcription-quantitative polymerase chain reaction (RT-qPCR). Total RNA was extracted from tissue and cells using the ultra-pure RNA extraction kit according to the manufacturer's instructions. RNA was then quantified using

Table I. Primer sequences.

Gene	Forward (5'-3')	Reverse (5'-3')
Mouse Cx43	ACAGGAGAGTGCCTTGGTAGTGAC	GTTGCTGGACTTGCTGGACCTTC
Mouse miR-206	GCTCGTGGAATGTAAGGAAGT	AGTGCAGGGTCCGAGGTATT
Mouse GAPDH	AACGGGAAGCCCATCACC	CAGCCTTGGCAGCACCAG
Rat Cx43	GGAAATCGAACGGCTGGGCGT	TCGCGTGAAGGGAAGAAGCGAT
Rat miR-206	GCGCGTGGAATGTAAGGAAGT	AGTGCAGGGTCCGAGGTATT
Rat GAPDH	TGATTCTACCCACGGCAAGTT	TGATGGGTTTCCCATTGATGA

Cx43, connexin 43; miR-206, microRNA-206.

the NanoDrop 1000 (Thermo Fisher Scientific, Inc.). Reverse transcription was carried out with FastQuant cDNA First Chain Synthesis kit from 2 μg of total RNA according to the manufacturer's instructions. qPCR was performed using SYBR Green and measured with ABI 7500 Real-Time PCR System. The primer sequences are listed in Table I. Thermocycling conditions were as follows: 95˚C for 15 min, and then 40 cycles of 95˚C for 10 sec, 65˚C for 32 sec. mRNA levels were quantified using the $2^{-\Delta\Delta Cq}$ method (15) and normalized to GAPDH.

Immunohistochemistry. The middle lobe of the right lung of each mouse was fixed in 4% paraformaldehyde at room temperature for 24 h. Samples were embedded in paraffin then cut into 0.5-0.8 μm sections, then deparaffinized using xylene. Samples underwent a gradient ethanol hydration then were blocked in 10% normal goat serum (Beijing Solarbio Biotechnology Co., Ltd.) at room temperature for 30 min. Tissue sections were incubated with primary antibody against Cx43 (1:100; cat. no 15386-1-AP) at 37˚C for 2 h. Samples were rinsed with PBS three times then incubated with horseradish peroxidase-labeled secondary antibody (1:50; cat. no. ZDR5306; OriGene Technologies, Inc.) at room temperature for 45 min. Samples were rinsed with PBS three times, 3,3'-diaminobenzidine staining was performed then samples were sealed with neutral gum. A fluorescence inverted microscope (IX51; Olympus Corporation) was used to observe samples.

Western blot analysis. The upper lobes of right lung were removed from the mice, then they were placed separately in a mortar and the total proteins were extracted with radioimmunoprecipitation assay lysate solution (cat. no. AR0102; Wuhan Boster Biotechnology Co., Ltd.). The total protein concentration was quantified using the BCA quantitative kit (cat. no. AR0146; Wuhan Boster Biotechnology Co., Ltd.). A total of 30 μg sample protein was loaded per lane and separated using SDS-PAGE on a 20% gel, then transferred to a polyvinylidene difluoride membrane. The membrane was blocked in 5% milk for 2 h at room temperature. Membranes were incubated with primary antibody against Cx43 (1:500) overnight at 4˚C. Membranes were rinsed with Tris-buffered saline and Polysorbate 20 three times then incubated with horseradish peroxidase-labeled secondary antibody GAPDH (1:5,000; cat. no. BSAP0063; Bioworld Technology, Inc.) for 2 h at room temperature. Samples were rinsed five times. Then protein bands were visualized using super-sensitive enhanced chemiluminescent solution (cat. no. AR1111; Wuhan Boster Biotechnology Co., Ltd.) and analyzed using the Molecular Imager® Gel Doc™ XR+ system (Bio-Rad Laboratories, Inc.).

Table II. Protein concentration in BALF and lung W/D ratio.

Group	W/D	Protein in BALF (mg/l)
Sham	5.0±0.3	4.1±0.9
CLP	11.7±0.5[a]	11.9±3.9[a]
Cx43-In	5.9±0.3[b]	6.3±2.0[b]
miR-206-Mi	6.4±0.6[b]	8.5±0.9[b]

Data are presented as mean ± standard deviation from five mice per group. [a]P<0.05 vs. sham; [b]P<0.05 vs. CLP. BALF, bronchoalveolar lavage fluid; W/D ratio, lung wet weight to dry weight; CLP, caecum ligation and perforation; Cx43-In, CLP+connexin 43 inhibitors; miR-206-Mi, CLP+miR-206 analogs.

Monolayer cell culture. Cell culture was performed as previously described (16). One day prior to transfection, $2x10^5$ cells were seeded in the upper chamber on a Transwell plate to form a monolayer. Samples were randomly divided into six groups: sham, CLP, Cx43-In, Cx43-NC (5'-UUCUCC GAACGUGUCACGUTTACGUGACACGUUCGGAGA ATT-3'), miR-206-Mi and miR-206-NC groups. Cx43 inhibitor (20 μmol/l) and 2 μl of Lipofectamine 2000 transfection reagent were diluted with 50 μl serum-free DMEM and gently mixed to form 100 μl of a siRNA and Lipofectamine 2000 complex at room temperature for 20 min, then the complex was added to the cells in the Cx43-In group. miR-206 mimic (20 μmol/l; 5 μl) and 2 μl of Lipofectamine 2000 transfection reagent were diluted in 50 μl serum-free DMEM, then gently mixed at room temperature for 20 min to make 100 μl of the mimic and Lipofectamine 2000 complex; the complex was then added to cells in the miR-206-Mi group. The sham group and CLP group were incubated in 100 μl DMEM at 37˚C for 24 h. Transfection success rate was demonstrated by measuring miR-206 and Cx43 mRNA expression. After 24 h, all groups were supplemented with DMEM containing LPS (100 μg/l) for 6 h except for the sham group which was supplemented with DMEM only.

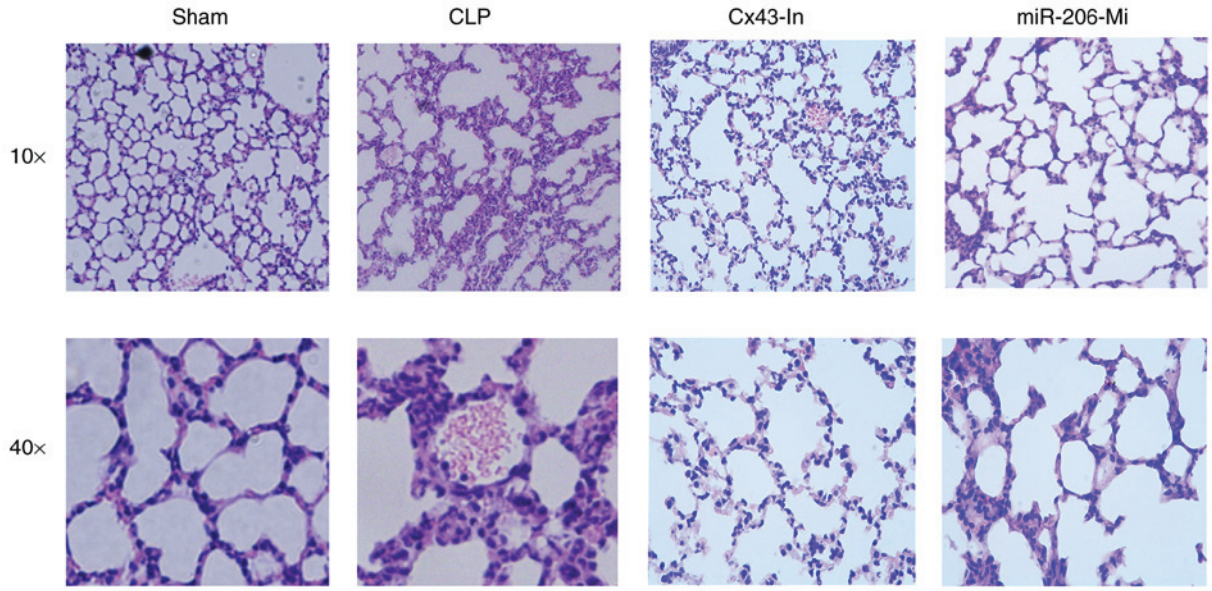

Figure 2. Hematoxylin and eosin staining of mouse lung tissue from sham, CLP, Cx43-In and miR-206-Mi groups. Micrographs demonstrate that mice from CLP, Cx43-In and miR-206-Mi groups displayed lung interstitial thickening, alveolar cavity edema and inflammatory cells infiltration (magnification, x100 and x400). CLP, caecum ligation and perforation; Cx43-In, CLP+connexin 43 inhibitors; miR-206-Mi, CLP+microRNA-206 analogs.

Permeability of monolayer cells. After 6 h of LPS stimulation and three PBS washes, 100 μl FITC-dextran (1 μg/ml) was added into the upper chamber and 600 μl sterile PBS was added into the lower chamber at 37ºC for 1 h. Cytation3 multi-function detection system (BioTek Instruments, Inc.) was used to test the absorbance value of FITC in the lower chamber. Results were displayed as a ratio of the experimental group to the control group.

Dual-luciferase reporter assay. miR-206 mimics (5'-UGGAAU GUAAGGAAGUGUGUGG-3') and miRNA-206-negative controls (NC; 5'-UUCUCCGAACGUGUCACGUTT-3') were synthesized, and the target sequence of the 3'UTR of the Cx43 gene was cloned into the on pmirGLO vector (Wuhan GeneCreate Biological Engineering Co., Ltd.). pmirGLO vector contained Firefly luciferase and *Renilla* luciferase as a control. The final transfected concentration was 0.97 μg/μl for the Cx43-wild-type (WT) plasmid, and 1.33 μg/μl for the Cx43-mutant (MT) plasmid. Cells (293T) were cultured in DMEM+FBS (10%) the day before transfection, so that the cell density at transfection was 70-80%. Firstly, 2 μl Lipofectamine 2000 transfection reagent was diluted in 50 μl serum-free DMEM; then plasmids and mimics were diluted in 50 μl serum-free DMEM (plasmid 1 μg; mimics 20 pmol). Lipofectamine 2000, and the plasmid and mimics solution (both 50 μl) were mixed at room temperature for 20 min, then 100 μl serum-free DMEM was added to form 200 μl transfection complex. Finally, the transfection complex was incubated with the cells at 37˚C for 5 h, then DMEM containing the transfection complex was removed. A total of 500 μl complete DMEM including 10% FBS without the transfection reagent was added and the cells were cultured at 37˚C for 48 h. Transfection was repeated for five times.

Detection of reporter gene expression intensity. Cell lysis solution (200 μl; cat. no. AR0102; Wuhan Boster Biotechnology Co., Ltd.) was added into each well of 293T cells and incubated at room temperature for 10 min. Following cell lysis, the solution was collected then centrifuged for 5 min at 10,000 x g/min (Avanti™J-30I; Beckman Coulter, Inc.) and the supernatant collected.

Firstly, firefly luciferase test reagent and *Renilla* luciferase test buffer from Luciferase Reporter Assay Kit (BioVision, Inc.) were defrosted at room temperature, and *Renilla* luciferase detection substrate (x100) was placed on in an ice box. In accordance with the manusfacturer's protocol, the chemiluminescence meter (BK-L96C; Beijing Binsino Biotechnology Co., Ltd.) was opened and 100 μl of the supernatant was added into the 96-well luminescence plate. The firefly luciferase detection working fluid (100 μl) was added, and the mixture was mixed. Finally, the luminescence value was measured on the computer; the integral time was 5 sec. The working fluid of 100 μl *Renilla* luciferase was added, and the luminescence value was measured on the computer after the mixture was mixed. The integral time was 5 sec. The relative light unit (RLU) value determined by *Renilla* luciferase was divided by the RLU value determined by firefly luciferase. The authors compared the activation degree of reporter gene between different samples according to the obtained ratio.

Statistical analysis. Data was processed using SPSS v19.0 (IBM Corp.). The data in this study were presented as mean ± standard error. Statistical significance was assessed using one-way analysis of variance followed by Fisher's least significant difference method for uniform variance and Dunnett's test for non-uniform variance. All experiments were repeated at least five times. $P<0.05$ was considered to indicate statistical significance.

Results

CLP induces a strong inflammatory response in mouse lung. The degree of damage to the alveolar structure was dependent on the treatment group, with the CLP group demonstrating

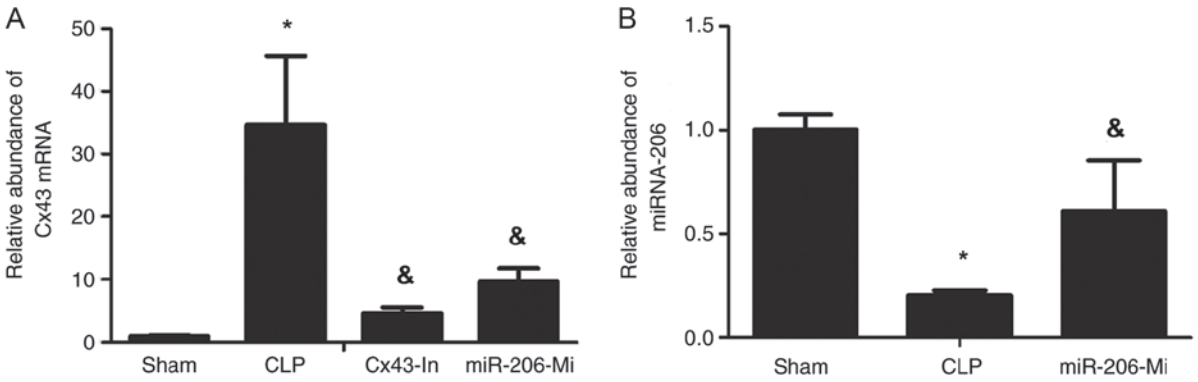

Figure 3. Successful transfection demonstrated by miR-206 and Cx43 mRNA expression. (A) Cx43 and (B) miR-206 mRNA expression levels were measured using reverse transcription-quantitative polymerase chain reaction. *P<0.05 vs. sham; &P<0.05 vs. CLP. miR-206, microRNA-206; Cx43, connexin 43; CLP, caecum ligation and perforation.

the most significant changes (Fig. 2). The CLP, Cx43-In and miR-206-Mi groups demonstrated alveolar wall thickening, pulmonary interstitium hyperemia and hemorrhage, inflammatory cells infiltration, pulmonary interstitium and alveolar space edema, alveolar cavities neutrophils and reddish edema fluid exudate (Fig. 2). There was no significant change in lung tissue in the sham group (Fig. 2). Compared with the CLP group, the inflammatory response was alleviated in the Cx43-In and miR-206-Mi groups.

miR-206 significantly decreases alveolar air-blood barrier permeability following sepsis-induced ALI. W/D of lung tissue reflected the degree of pulmonary edema and the protein content of BALF reflected the permeability of the alveolar air-blood barrier. At 6 h following modeling, the lung tissue water content and the concentration of protein in the BALF were significantly increased compared with the sham group (P<0.05; Table II). The water content of lung tissue and the protein concentration of BALF in the Cx43-In group and miR-206-Mi groups were significantly decreased compared to the CLP group (P<0.05; Table II).

miR-206 significantly decreases Cx43 mRNA expression following sepsis-induced ALI. Cx43 mRNA expression in the lung tissue of the CLP group was significantly increased compared with the sham group (P<0.05; Fig. 3A). Cx43 mRNA expression for the Cx43-In group and the miR-206-Mi group was decreased compared with the CLP group (P<0.05; Fig. 3A). The expression of miR-206 was significantly decreased in the CLP group compared with the sham group (P<0.05; Fig. 3B). The expression of miR-206 was increased in the miR-206-Mi group compared with the CLP group (P<0.05; Fig. 3B).

miR-206 decreases Cx43 protein expression following sepsis-induced ALI. Immunohistochemistry analysis demonstrated that Cx43 protein expression in the CLP group was significantly enhanced compared with the sham group (Fig. 4). Cx43 protein expression was decreased in the Cx43-In group and the miR-206-Mi group compared with the CLP group (Fig. 4).

These findings were further confirmed by western blot analysis. A presented in Fig. 5, Cx43 protein expression in the CLP group was significantly increased compared with the sham group (P<0.05). Compared with the CLP group, Cx43 protein expression in the Cx43-In group and the miR-206-Mi group was significantly decreased (P<0.05), but was still higher than the sham group (P<0.05; Fig 5).

miR-206 decreases the permeability of ATII monolayer following ALI induction. The permeability of the ATII monolayer in the CLP group was increased compared with the sham group (P<0.05; Fig. 6). Compared with the CLP group, the permeability of the ATII monolayer in the Cx43-In group and the miR-206-Mi group were significantly decreased (P<0.05; Fig. 6).

Successful transfection confirmed by Cx43 and miR-206 expression. Transfection success rate was demonstrated by RT-qPCR analysis for miR-206 and Cx43 mRNA expression. Cx43 mRNA expression in the CLP group was significantly increased compared with the sham group (P<0.05; Fig 7A). Cx43 mRNA expression in the Cx43-In group was significantly decreased compared with the CLP group (P<0.05; Fig 7A). Of note, the Cx43 mRNA expression was not significantly decreased in the miR-206-Mi group compared with the miR-206-NC (P>0.05; Fig 7A). Cx43 mRNA expression decreased in the Cx43-In group relative to the Cx43-NC group (P<0.05; Fig. 7A).

The expression of miR-206 was significantly decreased in the CLP group compared with the sham group (P<0.05; Fig. 7B). miR-206 expression was increased in the miR-206-Mi group compared with the CLP group (P<0.05; Fig. 7B). The expression of miR-206 in the miR-206-Mi group was increased relative to the miR-206-NC group (P<0.05; Fig. 7B).

miR-206 significantly decreases Cx63 protein expression in vitro. Cx43 protein expression in the CLP group was significantly increased compared with the sham group (P<0.05; Fig. 8). Cx43 protein expression in the Cx43-In group and the miR-206-Mi group was significantly lower compared with the CLP group (P<0.05; Fig. 8) but higher compared with the sham group (P<0.05; Fig. 8). Cx43 expression was lower in the Cx43-In group compared with the Cx43-NC group (P<0.05; Fig. 8). Cx43 expression in the miR-206-Mi group was lower compared with the miR-206-NC group (P<0.05; Fig. 8).

miR-206 interacts with the 3'UTR of Cx43. miRNA target gene prediction software TargetScan indicated that the 3'UTR of the Cx43 gene had 466-473 and 1580-1587 sequences

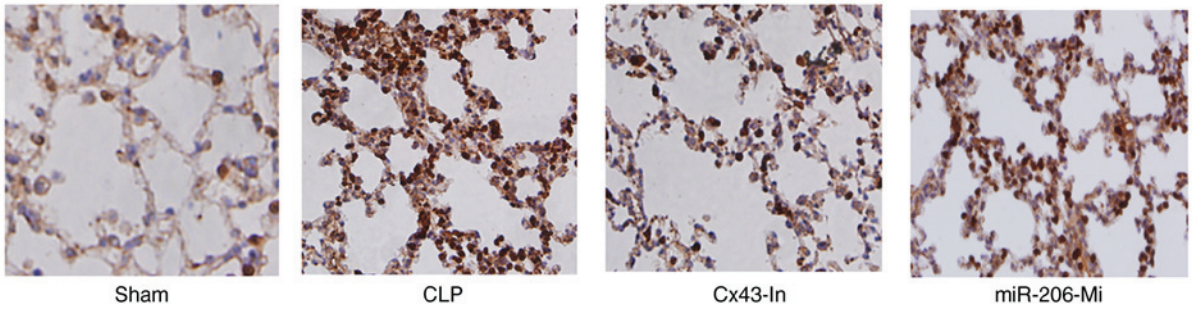

Figure 4. Immunohistochemistry micrographs for Cx63 protein expression in sham, CLP, Cx43-In and miR-206-Mi groups (magnification, x400). Cx43, connexin 43; CLP, caecum ligation and perforation; Cx43-In, CLP+connexin 43 inhibitors; miR-206-Mi, CLP+microRNA-206 analogs.

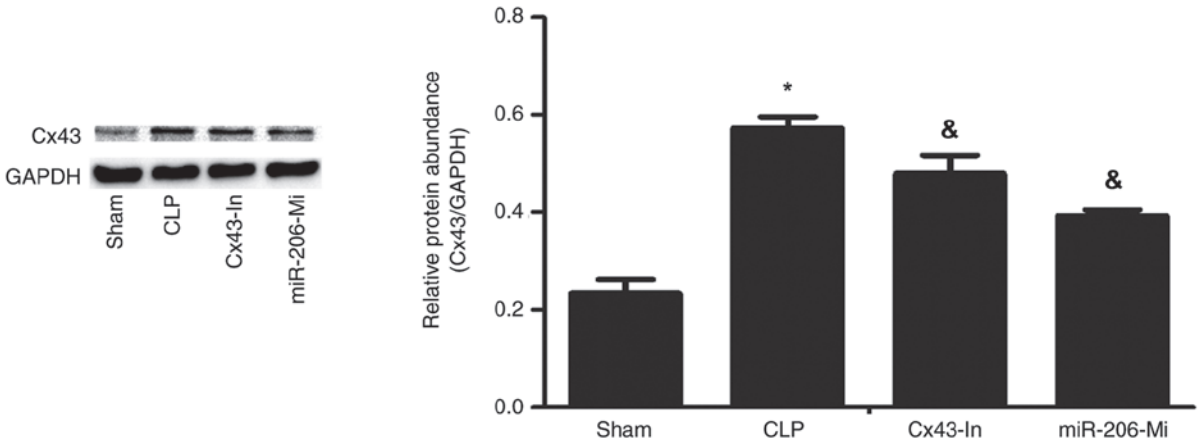

Figure 5. Protein expression of Cx43 in sham, CLP, Cx43-In and miR-206-Mi groups. Representative western blots and quantification against GAPDH. *P<0.05 vs. sham; &P<0.05 vs. CLP. Cx43, connexin 43; CLP, caecum ligation and perforation; Cx43-In, CLP+connexin 43 inhibitors; miR-206-Mi, CLP+microRNA-206 analogs.

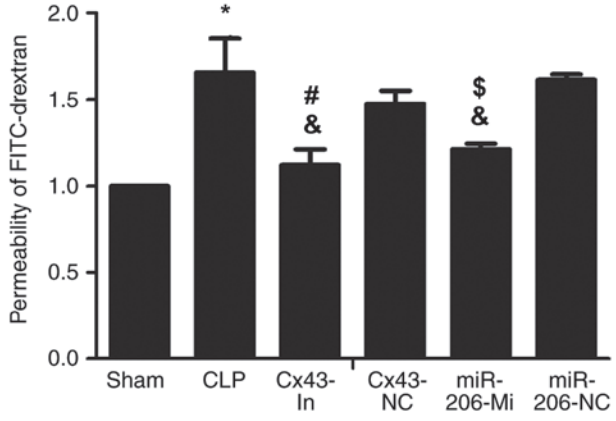

Figure 6. Permeability of monolayer ATII cells measured by FITC-dextran absorbance value. *P<0.05 vs. sham; &P<0.05 vs. CLP; #P<0.05 vs. Cx43-NC; $P<0.05 vs. miR-206-NC. ATII, alveolar type II epithelial; FITC, fluorescein isothiocyanate; CLP, caecum ligation and perforation; Cx43, connexin 43; NC, negative control; miR-206, microRNA-206; Cx43-In, CLP+connexin 43 inhibitors; miR-206-Mi, CLP+miR-206 analogs.

complementary to miR-206 (Fig. 9A). Fluorescence intensity was significantly downregulated compared with the control group following miR-206 and Cx43-WT transfection (P<0.05, Fig. 9B) which suggested that miRNA-206 interacted directly with the 3'UTR of Cx43.

Discussion

The present study determined that the alveolar air-blood barrier permeability was increased in sepsis-induced ALI mice, permeability of monolayer ATII cells was increased by LPS and Cx43 downregulation due to Cx43 mRNA inhibitors (antagomir) decreased permeability of ATII barrier. It was also demonstrated that Cx43 expression decreased following the application of miRNA-206 analogs (agomir) and the dual-luciferase report gene assay demonstrated that miR-206 targeted Cx43 mRNA 3'UTR to influence Cx43 mRNA translation.

HE staining, W/D and BALF protein content confirmed the establishment of a successful sepsis-induced ALI mouse model. HE staining revealed that the CLF method induced alveolar structure destruction, alveolar wall thickening, pulmonary interstitium hyperemia, interstitium hemorrhage, inflammatory cell infiltration, alveolar edema, reddish edema in the alveolar cavity, and neutrophils exudation, which is consistent with the previous literature (17). The W/D and BALF protein concentration in sepsis-induced ALI mice were also increased, further indicating successful modeling. Experiments were performed 6 h following modeling due to the inflammatory response peaking at this time point (18).

To explore the role of Cx43 in alveolar air-blood barrier permeability *in vitro*, ATII cells were cultured in monolayer. Following LPS stimulation, the monolayer permeability

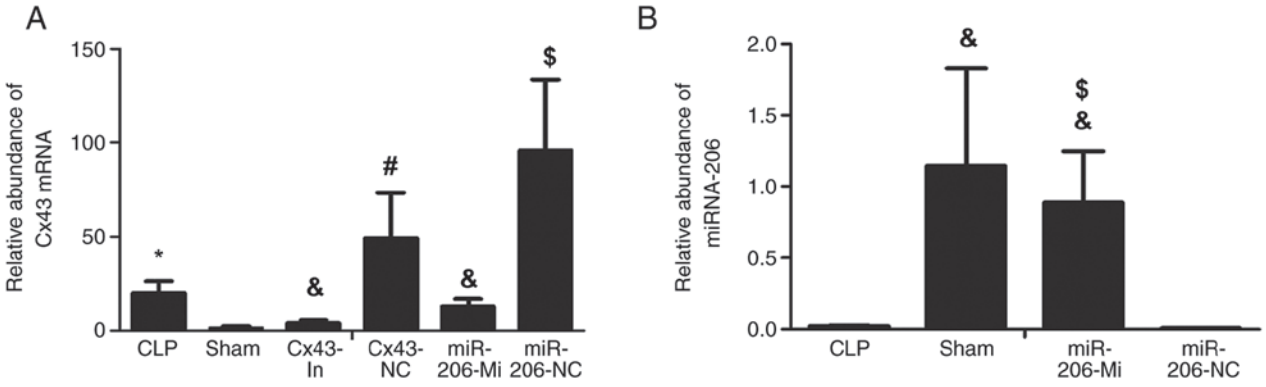

Figure 7. (A) Cx43 and (B) miR-206 gene expression measured by reverse transcription-quantitative polymerase chain reaction. *P<0.05 vs. sham; &P<0.05 vs. CLP; #P<0.05 vs. Cx43-NC; $P<0.05 vs. miR-206-NC. Cx43, connexin 43; miR-206, microRNA-206; CLP, caecum ligation and perforation; NC, negative control; Cx43-In, CLP+connexin 43 inhibitors; miR-206-Mi, CLP+miR-206 analogs.

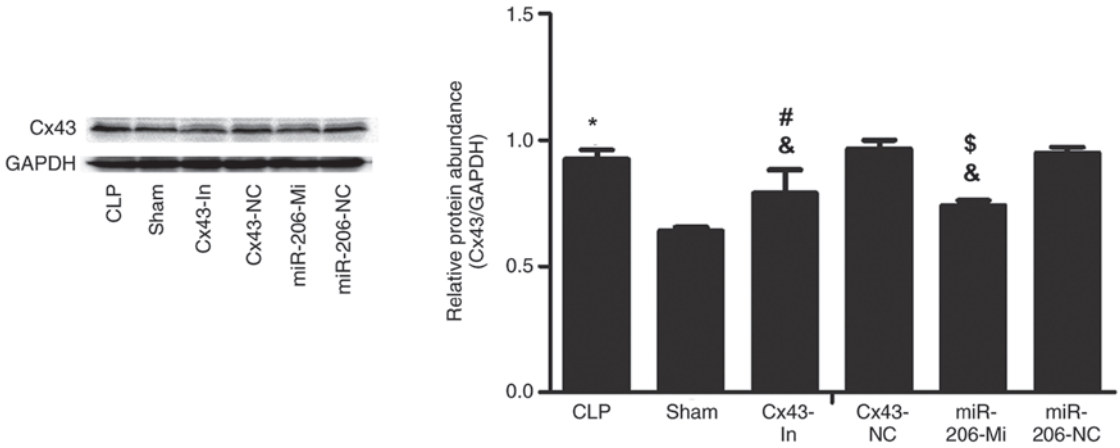

Figure 8. Cx43 protein expression determined using western blot analysis. *P<0.05 vs. sham; &P<0.05 vs. CLP; #P<0.05 vs. Cx43-NC; $P<0.05 vs. miR-206-NC.

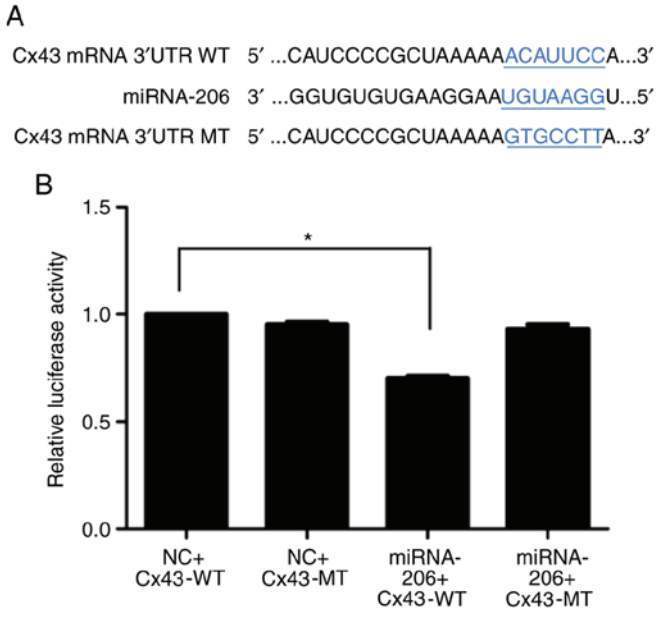

Figure 9. miR-206 directly targets the 3'UTR of Cx43. (A) 3'UTR of Cx43 mRNA is complementary with miR-206. The sequences highlighted in blue represent the nucleotides altered in order to generate the mutant reporter plasmid. (B) Dual-luciferase reporter gene experiment. *P<0.05 vs. control. UTR, untranslated region; Cx43, connexin 43; miR-206, microRNA-206; NC, negative control; WT, wild-type; MT, mutant.

increased significantly which is consistent with previous studies (4,5). This experiment demonstrated the important role of the ATII barrier in alveolar air-blood barrier permeability. Cx43 serves various roles in the development of different diseases. It has been reported that inhibition of miR-20, upregulates Cx43 expression which attenuates alkali burn-induced keratitis (19). Anderson *et al* (12) determined that miR-206 downregulates Cx43 expression which serves an important role in skeletal myoblast formation and differentiation. The present study demonstrated that the severity of sepsis-induced ALI was attenuated and the permeability of monolayer cells was decreased by using miR-206 mimics and Cx43 mRNA inhibitors. The important role of Cx43 in the alveolar air-blood barrier and the regulation of Cx43 expression by miRNAs were verified *in vivo* and *in vitro*. Finally, using dual luciferase reporter gene assay, it was determined that miR-206 affected the translation of Cx43 mRNA and downregulated Cx43 expression by targeting the 3'UTR of Cx43 mRNA.

The present study demonstrated the important role of ATII cells in the alveolar barrier permeability of sepsis-induced ALI; however, it has several limitations. The effects of pulmonary microvascular endothelial permeability on alveolar epithelial production were not studied *in vitro* or *in vivo* as the focus of this study was investigation into the role of ATII cells in alveolar air-blood barrier permeability. The mechanism of how

siRNA reached the alveolar epithelium through the air-blood barrier before modeling was also not explored although it was hypothesized that it may be related to the molecular weight and homology of the siRNA. Future study will include labeling siRNAs with fluorescent dyes to dynamically observe the migration process of the siRNAs. Also the regulation of Cx43 mRNA by miR-206 in human ATII cells by dual luciferase reporter gene assay and the relationship between Cx43 and alveolar air-blood barrier permeability in human A549 cells will be investigated.

In conclusion, the present study demonstrated that the permeability of the alveolar air-blood barrier in sepsis-induced ALI was positively correlated with Cx43 expressed by ATII cells. miR-206 was involved in the regulation of alveolar air-blood barrier permeability by regulating Cx43 expression. The present findings provide a potential novel approach for the treatment of sepsis-induced ALI.

Acknowledgements

Not applicable.

Funding

The present study was supported by grants from the Scientific Research Funding Project for Returnees in Shanxi Province of China (grant no. 2011-105) and the Taiyuan Science and Technology Project of Shanxi Province of China (grant no. 12016905).

Availability of data and materials

The datasets used and analyzed during the present study are available from the corresponding author on reasonable request.

Authors' contributions

KL cultured the cells. YMF prepared the animal models. LYH performed the immunohistochemistry, immunoblotting and reverse transcription-quantitative polymerase chain reaction analysis. JWZ and WKZ designed the experiments, anlaysed the data and wrote the manuscript. All authors read and approved the final manuscript.

Ethics approval and consent to participate

The present study was approved by the Animal Ethics Committee of the Second Hospital of Shanxi Medical University.

Patient consent for publication

Not applicable.

Competing interests

The authors declare that they have no competing interests.

References

1. Minamino T and Komuro I: Regeneration of the endothelium as a novel therapeutic strategy for acute lung injury. J Clin Invest 116: 2316-2319, 2006.
2. Berger G, Klorin G, Ismael-Badarneh R, Guetta J and Azzam ZS: The cellular mechanisms of lung edema clearance: Does the alveolar epithelium play a role? Harefuah 156: 663-665, 2017.
3. Gorin AB and Stewart PA: Differential permeability of endothelial and epithelial barriers to albumin flux. J Appl Physiol 47: 1315-1324, 1979.
4. Matthay MA, Cleriei C and Saumon G: Invited review: Active fluid clearance from the distal air spaces of the lung. J Appl Physilo 93: 1533-1541, 2002.
5. He ZG, Xiao N, Liu R, Tian KL, Diao YF and Fan XQ: Effects of endotoxin on the permeability of rat lung/intestinal microvesselS and cultured endothelial cells in vitro and the role apoptosis in the altered permeability. J Chin Med Res 5: 1214-1216, 2015 (In Chinese).
6. Johnson LN and Koval M: Cross-talk between pulmonary injury, oxidant stress, and gap junctional communication. Antioxid Redox Sign 11: 355-367, 2009.
7. Wu ZL, Liao CH and Ren N: Study on the correlation between connexin 43 and brain edema in experimental brain injury. Chin J Neurosurgery Dis Res 7: 201-204, 2012 (In Chinese).
8. Duan J, Zhang X, Zhang S, Hua S and Feng Z: MiR-206 inhibits FN1 expression and proliferation and promotes apoptosis of rat type II alveolar epithelial cells. Exp Ther Med 13: 3203-3208, 2017.
9. Radzikinas K, Aven L, Jiang Z, Tran T, Paez-Cortez J, Boppidi K, Lu J, Fine A and Ai X: A Shh/miR-206/BDNF cascade coordinates innervation and formation of airway smooth muscle. J Neurosci 31: 15407-15415, 2011.
10. Zhang H, Guo Y, Mishra A, Gou D, Chintagari NR and Liu L: MicroRNA-206 regulates surfactant secretion by targeting VAMP-2. FEBS Lett 589: 172-176, 2015.
11. Lin ZJ, Ming J, Yang L, Du JZ, Wang N and Luo HJ: Mechanism of regulatory effect of microRNA-206 on connexin 43 in distant metastasis of breast cancer. Chin Med J 129: 424-434, 2016.
12. Anderson C, Catoe H and Werner R: MiR-206 regulates connexin 43 expression during skeletal muscle development. Nucleic Acids Res 34: 5863-5871, 2006.
13. Kim HK, Lee YS, Sivaprasad U, Malhotra A and Dutta A: Muscle-specific microRNA miR-206 promotes muscle differentiation. J Cell Biol 174: 677-687, 2006.
14. Zahar JR, Timsit JF, Garrouste-Orgeas M, Francais A, Vesin A, Descorps-Declere A, Dubois Y, Souweine B, Haouache H, Goldgran-Toledano D, *et al*: Outcomes in severe sepsis and patients with septic shock: Pathogen species and infection sites are not associated with mortality. Crit Care Med 39: 1886-1895, 2011.
15. Livak KJ and Schmittgen TD: Analysis of relative gene expression data using real-time quantitative PCR and the 2(-Delta Delta C(T)) methods. Method 25: 402-408, 2001.
16. Fan Y, Wu DZ, Gong YQ, Zhou JY and Hu ZB: Effects of calycosin on the impairment of barrier function induced by hypoxia in human umbilical vein endothelial cells. Eur J Pharmacol 481: 33-40, 2003.
17. Zhang JF, Zhang ZQ, Luo XT, Hou LY, Jiang Q, Lv JP and Zhang WK: Bone marrow mesenchymal stem cells regulate nuclear factor kappaB expression in alveolar macrophages of acute lung injury rats with sepsis. Chin J Tissue Engineering Res 19: 1556-1561, 2015 (In Chinese).
18. Zhang F, Li ZL, Shi Y, Zhao M, Xin XF and Qian GS: Nuclear factor κB in LPS stimulated rat alveolar macrophages promotes TNF-A secretion. Chin J Pathophysiol 23: 1412-1414, 2007.
19. Li XY, Zhou HF, Tang WQ, Guo Q and Zhang Y: Transient downregulation of microRNA-206 protects alkali burn injury in mouse cornea by regulating connexin 43. Int J Clin Exp Pathol 8: 2719-2727, 2015.